Available online at www.sciencedirect.com

SciVerse ScienceDirect

Ceramics International 39 (2013) 1397–1402

CERAMICS INTERNATIONAL

www.elsevier.com/locate/ceramint

Electrical conductivity and thermoelectric power studies of solution-combustion-processed $Ca_{2.76}Cu_{0.24}Co_4O_9$

G.W. Lee[a], J.Y. Kim[a], T. Athar[a], S.J. Kim[a], W.S. Seo[b], K. Park[a,*]

[a]*Faculty of Nanotechnology and Advanced Materials Engineering, Sejong University, Seoul 143-747, Republic of Korea*
[b]*Korea Institute of Ceramic Engineering and Technology, Seoul 153-023, Republic of Korea*

Received 16 February 2012; received in revised form 24 July 2012; accepted 24 July 2012
Available online 1 August 2012

Abstract

Nanocrystalline $Ca_{2.76}Cu_{0.24}Co_4O_9$ powders (25 nm in crystallite size) are synthesized by the solution combustion method, using aspartic acid as the combustion fuel. In this study, we discuss the effect of sintering temperature on the microstructure and thermoelectric properties of $Ca_{2.76}Cu_{0.24}Co_4O_9$. The density and grain size increase with an increase in sintering temperature. The $Ca_{2.76}Cu_{0.24}Co_4O_9$ sintered at 900 °C shows the largest value of electrical conductivity and Seebeck coefficient, resulting in the largest power factor (3.8×10^{-4} W m^{-1} K^{-2} at 800 °C). This value is more than 22 times larger than that of the $Ca_{2.76}Cu_{0.24}Co_4O_9$ sintered at 940 °C (1.7×10^{-5} W m^{-1} K^{-2} at 800 °C).

Keywords: Powders: Chemical preparation; Electron microscopy; Electrical conductivity; Functional applications

1. Introduction

Thermoelectric power generation converts thermal energy directly into electrical energy via the Seebeck effect induced by a temperature difference in solid materials. Thermoelectric materials are solid-state energy converters in which a combination of electrical and thermal properties allows them to be utilized in order to convert waste heat into electricity or electrical energy directly into cooling and heating [1]. As a result, thermoelectric materials have attracted considerable interest as a clean energy-conversion system in harmony with the environment. The performance of thermoelectric materials is usually evaluated in terms of their thermoelectric figure-of-merit Z, which can be expressed by the following equation:

$$Z = \frac{\sigma\alpha^2}{\kappa} \qquad (1)$$

where σ, α, and κ are the electrical conductivity, the Seebeck coefficient, and the thermal conductivity, respectively. For a large Z value, it is necessary to obtain a high Seebeck coefficient, a high electrical conductivity, and a low thermal conductivity.

As strong electron correlation systems, cobaltites such as $Na_xCo_2O_4$ and $Ca_3Co_4O_9$ exhibit the coexistence of a large Seebeck coefficient and a low electrical resistivity, which allows them to be attractive candidates for thermoelectric application [2]. A great deal of attention has especially been given to $Ca_3Co_4O_9$ due to its high value of figure-of-merit and excellent thermal and chemical stability at high temperatures in air [3–6]. The oxide consists of alternating single CdI_2-type CoO_2 layers and triple rock-salt-type Ca_2CoO_3 layers along the *c*-axis [7]. The CoO_2 layers in $Ca_3Co_4O_9$, which consist of an edge-sharing octahedral with a small distortion, are conducting planes, significantly contributing to electrical conduction as well as large thermoelectric power [8]. The Ca_2CoO_3 layers consist of two Ca–O planes and one Co–O plane, with the Ca–O planes playing the role of donors to the CoO_2 layers [9]. As a result, a misfit-layer $Ca_3Co_4O_9$ shows highly anisotropic properties and charge carrier transport is mainly restricted to the CoO_2 planes.

It has been reported that the thermoelectric properties of $Ca_3Co_4O_9$ are improved by partially substituting Na, K, La, Sr, Gd, or Y for Ca as well as Ni, Fe, Mn, or Cu for Co in $Ca_3Co_4O_9$ [2,4–6,9–12]. The charge carriers can

*Corresponding author. Tel.: +82 2 3408 3777; fax: +82 2 3408 4342.
E-mail address: kspark@sejong.ac.kr (K. Park).

0272-8842/$ - see front matter
http://dx.doi.org/10.1016/j.ceramint.2012.07.081

change over a wide range by doping so that the effective valence of Co ions changes from Co^{2+} to Co^{4+} in $Ca_3Co_4O_9$ [2]. In the present study, we substitute Cu for Ca in $Ca_3Co_4O_9$. It is also known that controlling the process, especially sintering, is a promising route for improving thermoelectric properties [13,14]. In this work, we fabricate $Ca_{2.76}Cu_{0.24}Co_4O_9$ at various sintering temperatures (860–940 °C), using the solution combustion-processed $Ca_{2.76}Cu_{0.24-}Co_4O_9$ powders. The solution combustion method is considered an attractive for synthesizing pure and nanocrystalline oxide-based powders within a short period of time [15,16]. Subsequently, we systematically investigate the effect of sintering temperature on thermoelectric properties.

2. Experimental

To synthesize $Ca_{2.76}Cu_{0.24}Co_4O_9$ powders, aspartic acid ($C_4H_7NO_4$) was employed as the combustion fuel, and $Ca(NO_3)_2 \cdot xH_2O$, $Co(NO_3)_2 \cdot 6H_2O$, and $Cu(NO_3)_2 \cdot 6H_2O$ nitrates were utilized as oxidizers. The solution combustion process took place through the reaction of the nitrates and the fuel. An appropriate proportion of the nitrates was dissolved in distilled water. The nitrates-to-aspartic acid ratio in the precursor solution was adjusted to 1:1. The mixed aqueous solutions of the nitrates and aspartic acid were heated slowly on a hot plate until they became viscous gel precursors. After a strong, rapid and exothermic reaction, voluminous $Ca_{2.76}Cu_{0.24}Co_4O_9$ powders were acquired.

The morphological characteristics of the synthesized powders were investigated with a field emission scanning electron microscope (FE-SEM; Hitachi S4700). The synthesized powders were ground and then investigated with a transmission electron microscope (TEM; JEOL JEM-2100F, Japan) operating at 200 kV. The resultant powders were calcined at 800 °C for 12 h. Subsequently, the calcined powders were cold-pressed under 150 MPa to prepare green pellets. The green compacts were heated in air to 860–940 °C at a rate of 5 °C min^{-1} and kept at that temperature for 24 h for sintering, and then furnace cooled to room temperature.

The crystal structure of the synthesized and sintered $Ca_{2.76}Cu_{0.24}Co_4O_9$ samples was analyzed with an X-ray diffractometer (XRD; Rigaku DMAX 2500) using Cu Kα radiation at 40 kV and 100 mA. The microstructure of the sintered samples was investigated with a field emission scanning electron microscope (FE-SEM, Hitachi S-4700). The density of the sintered samples was measured by the Archimedes method.

We simultaneously measured the electrical conductivity (σ) and the Seebeck coefficient (α) over the temperature range 500–800 °C. The samples for the measurements of thermoelectric properties were polished out of the sintered bodies in the form of rectangular bars of 2 mm × 2 mm × 15 mm. Four grooves were put on the rectangular bars, and Pt wires were wound along the grooves. Holes (~1.0 mm in diameter) were machined in the middle of the two end grooves in the samples. The insulated heads of the two Pt/Pt-Rh (13%) thermocouples were embedded in the two holes, and the temperatures at the holes were measured. The electrical conductivity was measured using the direct-current (DC) four-probe method. For thermopower measurements, a temperature difference was generated in the sample by passing cool Ar gas over one end of the sample placed inside a quartz protection tube. The temperature difference between the two ends of the sample was controlled at 4–6 °C using a flowmeter to vary flow rate of the Ar gas. The thermoelectric voltage ΔE measured as a function of the temperature difference ΔT showed a straight line. The Seebeck coefficient α was calculated from the relation $\alpha = \Delta E/\Delta T$.

3. Results and discussion

$Ca_{2.76}Cu_{0.24}Co_4O_9$ thermoelectric samples are fabricated by the solid-state reaction method, using solution combustion-processed $Ca_{2.76}Cu_{0.24}Co_4O_9$ powders. The following reaction is considered for the synthesis of $Ca_{2.76}Cu_{0.24}Co_4O_9$ powders:

$$\frac{69}{25}Ca(NO_3)_2xH_2O+\frac{6}{25}Cu(NO_3)_2\cdot 6H_2O$$
$$+4Co(NO_3)_2\cdot 6H_2O+\frac{14}{3}C_4H_7NO_4+O_2$$
$$\rightarrow Ca_{2.76}Cu_{0.24}Co_4O_9+\frac{28}{3}N_2+\frac{56}{3}CO_2+\left(\frac{67}{3}+x\right)H_2O$$

Fig. 1 shows FE-SEM images of the synthesized $Ca_{2.76}Cu_{0.24}Co_4O_9$ powders. The images exhibit porous and sponge-like agglomerated powders. These morphological

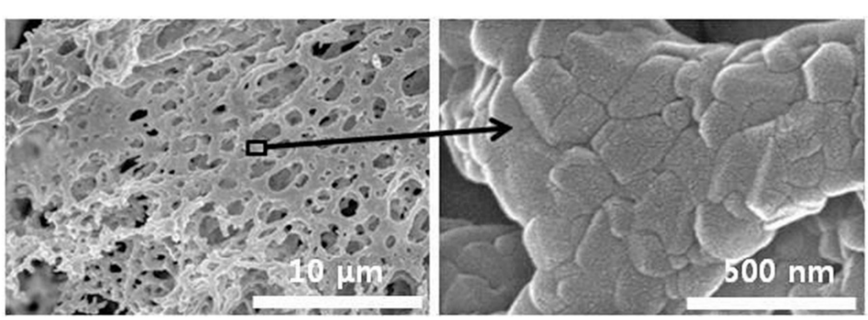

Fig. 1. FE-SEM images from the synthesized $Ca_{2.76}Cu_{0.24}Co_4O_9$ powders.

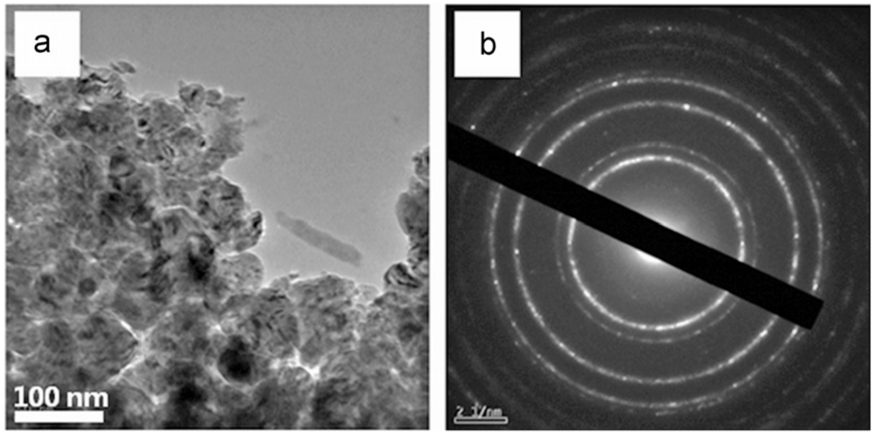

Fig. 2. (a) TEM bright field image and (b) its corresponding SAED pattern from the synthesized $Ca_{2.76}Cu_{0.24}Co_4O_9$ powders.

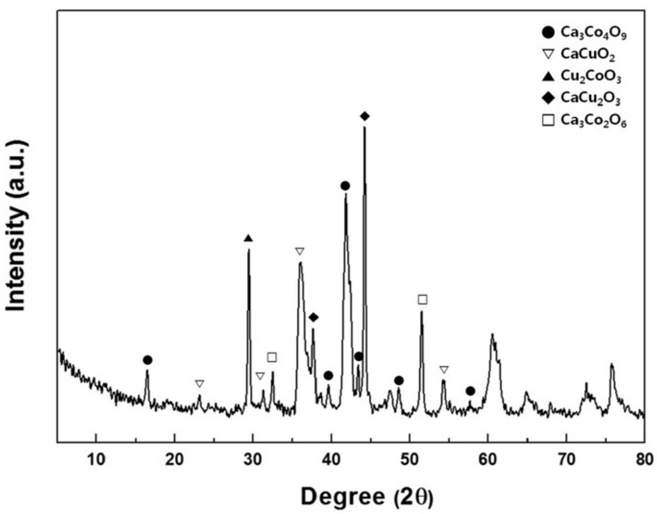

Fig. 3. XRD pattern from the synthesized $Ca_{2.76}Cu_{0.24}Co_4O_9$ powders.

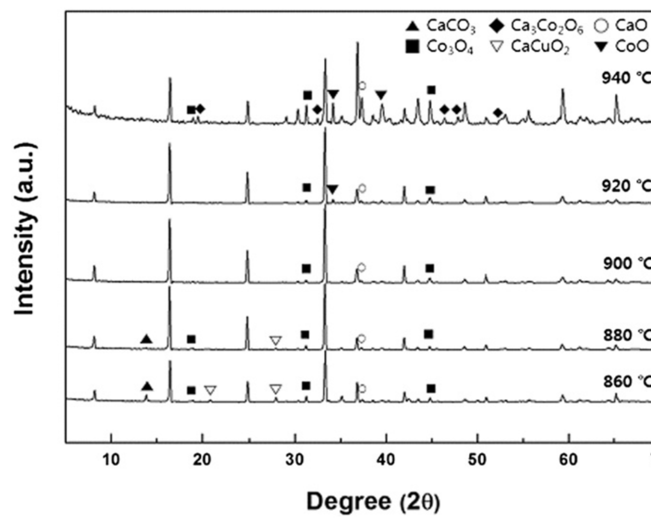

Fig. 4. XRD patterns from the $Ca_{2.76}Cu_{0.24}Co_4O_9$ pellets sintered at different temperatures (860–940 °C).

characteristics are attributed to the liberation of a large amount of gas during the combustion of gels. A typical TEM bright field image and its corresponding selected area electron diffraction (SAED) pattern from the synthesized $Ca_{2.76}Cu_{0.24}Co_4O_9$ powders are shown in Fig. 2(a) and (b), respectively. The synthesized $Ca_{2.76}Cu_{0.24}Co_4O_9$ powders show a nanocrystalline nature.

This combustion processing for preparing $Ca_{2.76}Cu_{0.24}Co_4O_9$ nanopowders is an extremely simple and cost-effective method with improved powder characteristics in a short time, compared to conventional solid-state reaction processing [15,16]. The nucleation process during combustion occurs by the rearrangement and short-distance diffusion of atoms or molecules within a few seconds, which are responsible for the synthesis of nano-sized powders [18]. The XRD pattern of the synthesized $Ca_{2.76}Cu_{0.24}Co_4O_9$ powders is shown in Fig. 3. In addition to the $Ca_{2.76}Cu_{0.24}Co_4O_9$ solid solution, the synthesized powders contain $CaCuO_2$, Cu_2CoO_3, $CaCu_2O_3$, $Ca_3Co_2O_6$, and unidentified phases. The crystallite size (D) is calculated from the Scherrer formula

$$D = \frac{0.9\lambda}{\beta \cos\theta} \tag{2}$$

where λ is the wavelength of radiation, θ is the angle of the diffraction peak, and β is the full width at half maximum of the diffraction peak (in radian) [17]. The calculated size of the crystallite is 25 nm.

Fig. 4 shows the XRD patterns of the $Ca_{2.76}Cu_{0.24}Co_4O_9$ pellets sintered at different temperatures (860–940 °C). The major phase of the $Ca_{2.76}Cu_{0.24}Co_4O_9$ bodies is a solid solution of the constituents, which has a monoclinic symmetry [19]. In addition to the solid solution, the $Ca_{2.76}Cu_{0.24}Co_4O_9$ sintered at 860–880 °C contains small amounts of secondary phases such as $CaCO_3$, Co_3O_4, $CaCuO_2$, and CaO. The amount of these secondary phases decreases with an increase in sintering temperature. The $Ca_{2.76}Cu_{0.24}Co_4O_9$ sintered at 900 °C contains secondary phase Co_3O_4 and CaO. In addition, the $Ca_{2.76}Cu_{0.24}Co_4O_9$ sintered at 940 °C contains secondary phase Co_3O_4, CaO,

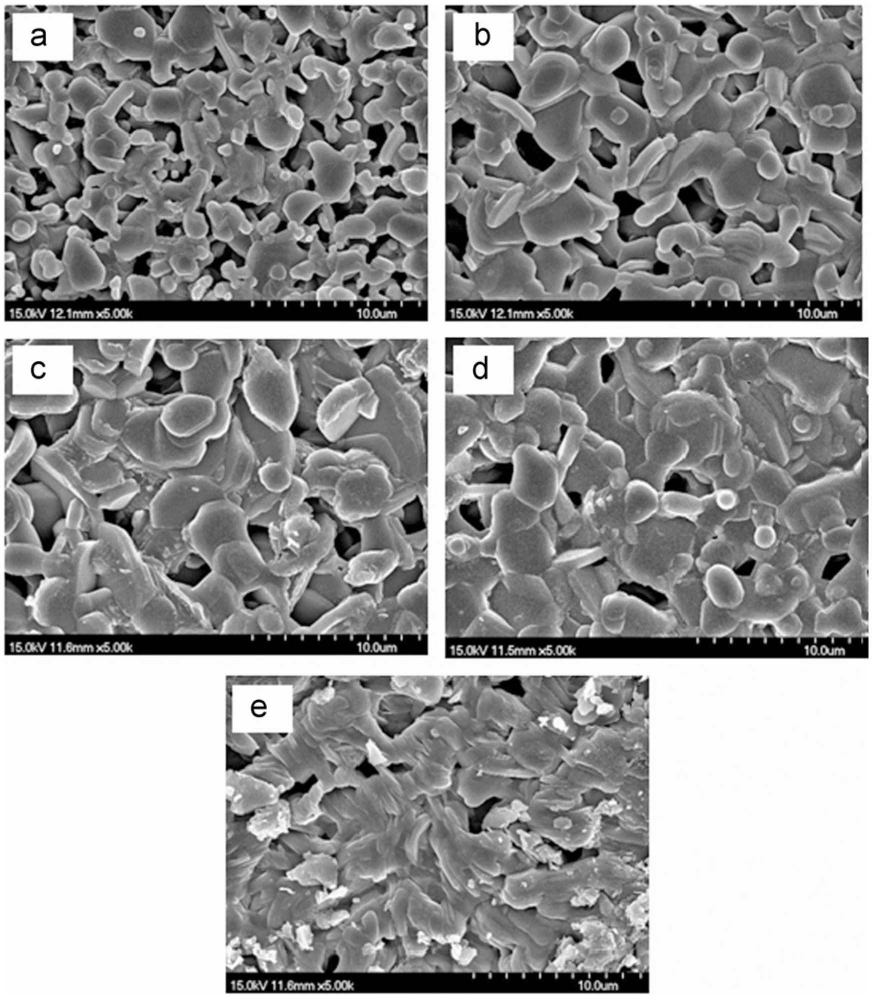

Fig. 5. FE-SEM images of the $Ca_{2.76}Cu_{0.24}Co_4O_9$ pellets sintered at (a) 860, (b) 880, (c) 900, (d) 920, and (e) 940 °C.

$Ca_3Co_2O_6$, and CoO [20]. The FE-SEM images of the $Ca_{2.76}Cu_{0.24}Co_4O_9$ pellets sintered at different temperatures (860–940 °C) are shown in Fig. 5. As expected, the density and grain size increase with a rise in sintering temperature. The densities of the $Ca_{2.76}Cu_{0.24}Co_4O_9$ pellets sintered at 860, 880, 900, 920, and 940 °C are 2.9, 3.3, 3.4, 3.7 and 3.8 g cm^{-3}, respectively, and the grain sizes of the $Ca_{2.76}Cu_{0.24}Co_4O_9$ pellets sintered at 860, 880, 900, 920, and 940 °C are 1.3, 2.1, 2.4, 3.1, and 3.6 μm, respectively.

The electrical conductivity (σ) of the $Ca_{2.76}Cu_{0.24}Co_4O_9$ samples sintered at 860–940 °C is plotted in Fig. 6. It is found that the electrical conductivity gradually increases with an increase in temperature, indicating a semiconducting behavior. The electrical conductivity (σ) can be expressed by the following equation:

$$\sigma = ne\mu \quad (3)$$

where n is the carrier density, e is the charge of carrier, and μ is the carrier mobility. We can assume that the substitution of Cu for Ca does not affect the carrier density because the content of Cu (0.24) in $Ca_{2.76}Cu_{0.24}Co_4O_9$ is constant. The sintering temperature affects the mobility and electrical conductivity. It is found that an increase in sintering temperature up to 900 °C yields a significant increase in the electrical conductivity. This is mainly attributed to an increase in grain size and density as well as to a decrease in

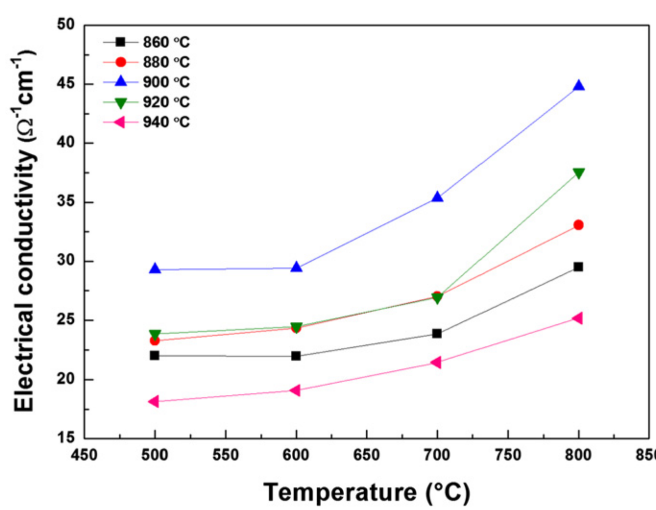

Fig. 6. Electrical conductivity of the $Ca_{2.76}Cu_{0.24}Co_4O_9$ samples sintered at 860–940 °C.

the secondary phases such as $CaCO_3$, Co_3O_4, $CaCuO_2$, and CaO. The grain boundary and pore act as scattering sites for conduction electrons. The higher the sintering temperature, the smaller the grain boundary area and porosity, thus increasing the electrical conductivity [21]. For the samples sintered at higher temperatures (920–940 °C), the electrical conductivity decreases with increasing sintering temperatures because of the formation of CoO and the increase of Co_3O_4. The highest value of the conductivity (44.8 Ω^{-1} cm^{-1} at 800 °C) is obtained for the $Ca_{2.76}Cu_{0.24}Co_4O_9$ sintered at 900 °C. This value is much larger than that of the $Ca_{2.76}Cu_{0.24}Co_4O_9$ sintered at 940 °C (25.2 Ω^{-1} cm^{-1} at 800 °C).

The Seebeck coefficient (α) as a function of temperature for the $Ca_{2.76}Cu_{0.24}Co_4O_9$ samples is shown in Fig. 7. The Seebeck coefficient increases with an increase in sintering temperature up to 900 °C, and then decreases with a further increase in sintering temperature. For the $Ca_{2.76}Cu_{0.24}Co_4O_9$ sintered at 900 °C, the value of the Seebeck coefficient is 293 μV K^{-1} at 800 °C. This value is more than three times as large as that of the $Ca_{2.76}Cu_{0.24}Co_4O_9$ sintered at 940 °C (82 μV K^{-1} at 800 °C). The temperature dependence of both the electrical conductivity and the Seebeck coefficient observed in this study is not explained by the conventional model based on band theory [22]. According to the conventional model, the value of the Seebeck coefficient decreases with increasing electrical conductivity. According to the Mott formula originated from the Sommerfeld expansion, the Seebeck coefficient can be expressed as follows [23]:

$$\alpha = \frac{c_e}{n} + \frac{\pi^2 \kappa_B^2 T}{3e}\left[\frac{\partial \ln\mu(\varepsilon)}{\partial\varepsilon}\right]_{\varepsilon=\varepsilon_F} \tag{4}$$

where c_e is the specific heat and is given by $c_e=(\pi^2\kappa_B^2 T/3e)\Psi(\varepsilon)$. And n, $\mu(\varepsilon)$, κ_B, and $\Psi(\varepsilon)$ are carrier concentration, energy correlated carrier mobility, Boltzmann constant, and density of state, respectively. Since the substitution of Cu scarcely affects the carrier density, as discussed previously, the second term of Eq. (4) dominates the Seebeck coefficient of $Ca_{2.76}Cu_{0.24}Co_4O_9$. However, the explanation of this phenomenon is unclear at the moment, and more data has to be gained from further experiments.

The temperature dependence of the power factor ($\sigma\alpha^2$) is shown in Fig. 8. The power factor of all the $Ca_{2.76}Cu_{0.24}Co_4O_9$ samples monotonically increases up to 800 °C. In addition, the power factor increases with sintering temperature up to 900 °C because of an increase in both the electrical conductivity and the Seebeck coefficient. At 800 °C, the power factor of the $Ca_{2.76}Cu_{0.24}Co_4O_9$ sintered at 900 °C (3.8×10^{-4} W m^{-1} K^{-2}) is more than 22 times larger than that of the $Ca_{2.76}Cu_{0.24}Co_4O_9$ sintered at 940 °C (1.7×10^{-5} W m^{-1} K^{-2}). In this respect, we need to precisely control the sintering temperature of $Ca_{2.76}Cu_{0.24}Co_4O_9$. The value of the power factor of the $Ca_{2.76}Cu_{0.24}Co_4O_9$ still increases toward higher temperatures, implying a high performance and stability at high temperatures.

In this work, we obtained porous structure in the $Ca_{2.76}Cu_{0.24}Co_4O_9$. It has been known that in addition to a high electrical conductivity and a high Seebeck coefficient, high-efficiency thermoelectric materials possess a low thermal conductivity to prevent a significant portion of the heat from flowing down the temperature gradient [24]. The thermal transport properties of thermoelectric materials are generally understood by means of the flow of carriers and heat-carrying phonons under the influence of the applied electric field and temperature gradient [24]. Pores in the thermoelectric materials significantly influence the electronic and lattice thermal conductivities since they significantly scatter carriers and heat-carrying phonons [25,26]. The porous $Ca_{2.76}Cu_{0.24}Co_4O_9$ fabricated here can reduce the two components of the thermal conductivity due to the effect of enhanced scattering of carriers and phonons by pores. Also, the porous structure usually plays an important role in heat transport and reduces the loss of heat by conduction. Experiments on Al-doped SiC showed

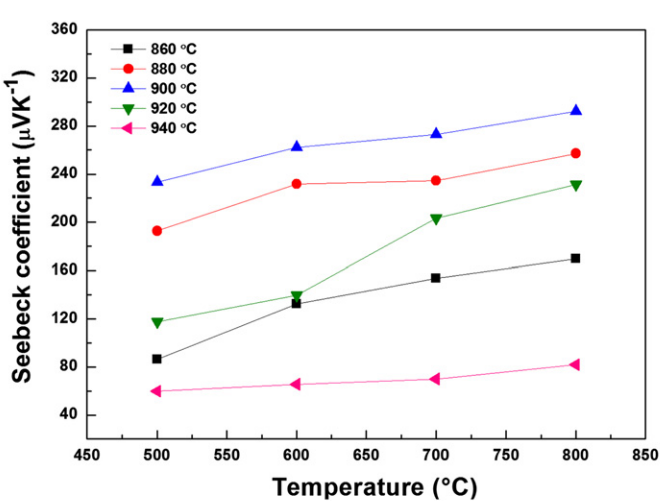

Fig. 7. Seebeck coefficient of the $Ca_{2.76}Cu_{0.24}Co_4O_9$ samples sintered at 860–940 °C.

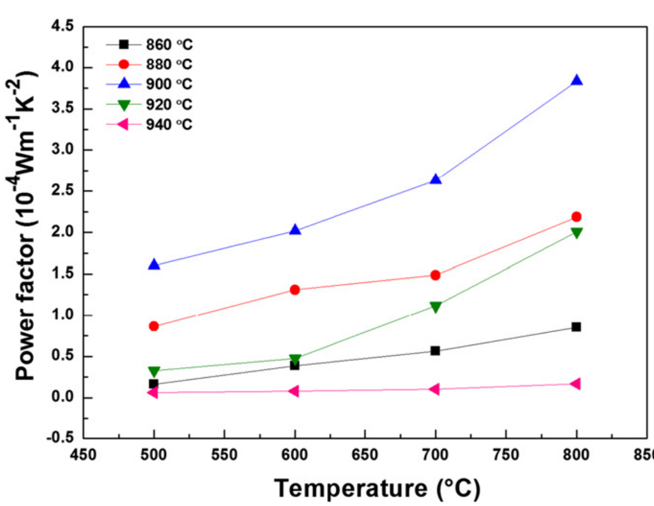

Fig. 8. Power factor of the $Ca_{2.76}Cu_{0.24}Co_4O_9$ samples sintered at 860–940 °C.

a pronounced decrease in the thermal conductivity due to the presence of pores. The thermal conductivity of Al-doped SiC was greatly decreased with an increase of porosity [27]. It is thus believed that the porous $Ca_{2.76}Cu_{0.24}Co_4O_9$ is favorable for decreasing the thermal conductivity, thereby improving energy conversion efficiency.

4. Conclusion

We synthesized nanocrystalline $Ca_{2.76}Cu_{0.24}Co_4O_9$ powders (25 nm in crystallite size) via the solution combustion method, using aspartic acid as the combustion fuel. An increase in sintering temperature led to a significant increase in the density and grain size. The electrical conductivity and the Seebeck coefficient increased with an increase in sintering temperature up to 900 °C, and then decreased with a further increase in sintering temperature. At 800 °C, the power factor of the $Ca_{2.76}Cu_{0.24}Co_4O_9$ sintered at 900 °C (3.8×10^{-4} W m^{-1} K^{-2}) was more than 22 times as large as that of the $Ca_{2.76}Cu_{0.24}Co_4O_9$ sintered at 940 °C (1.7×10^{-5} W m^{-1} K^{-2}). It was thus important to precisely control the sintering temperature of $Ca_{2.76}Cu_{0.24}Co_4O_9$.

Acknowledgment

This work is the outcome of a Manpower Development Program for Energy & Resources supported by the Ministry of Knowledge and Economy (MKE), Republic of Korea.

References

[1] L.E. Bell, Cooling, heating, generating power, and recovering waste heat with thermoelectric systems, Science 12 (2008) 1457–1461.
[2] Y. Wang, Y. Sui, P. Ren, L. Wang, X. Wang, W. Su, H. Fan, Strongly correlated properties and enhanced thermoelectric response in $Ca_3Co_{4-x}M_xO_9$ (M = Fe, Mn, and Cu), Chemistry of Materials 22 (2010) 1155–1163.
[3] J.G. Noudem, A new process for lamellar texturing of thermoelectric $Ca_3Co_4O_9$ oxides by spark plasma sintering, Journal of the European Ceramic Society 29 (2009) 2659–2663.
[4] S. Li, R. Funahashi, I. Matsubara, H. Yamada, K. Ueno, S. Sodeoka, Synthesis and thermoelectric properties of the new oxide ceramics $Ca_{3-x}Sr_xCo_4O_{9+\delta}$ ($x = 0.0-1.0$), Ceramics International 27 (2001) 321–324.
[5] J. Nan, J. Wu, Y. Deng, C.W. Nan, Synthesis and thermoelectric properties of $(Na_xCa_{1-x})_3Co_4O_9$ ceramics, Journal of the European Ceramic Society 23 (2003) 859–863.
[6] J. Nan, J. Wu, Y. Deng, C.W. Nan, Thermoelectric properties of La-doped Ca–Co–O misfit cobaltites, Solid State Communications 124 (2002) 243–246.
[7] Y. Masuda, D. Nagahama, H. Itahara, T. Tani, W.S. Seo, K. Koumoto, Thermoelectric performance of Bi- and Na-substituted $Ca_3Co_4O_9$ improved through ceramic texturing, Journal of Materials Chemistry 13 (2003) 1094–1099.
[8] K. Deshpande, A. Mukasyan, A. Varma, High-temperature electrical transport and thermoelectric power of partially substituted $Ca_3Co_4O_9$-based ceramics, Chemistry of Materials 16 (2004) 4896–4904.
[9] D. Li, X.Y. Qin, Y.J. Gu, J. Zhang, The effect of Mn substitution on thermoelectric properties of $Ca_3Mn_xCo_{4-x}O_9$ at low temperatures, Solid State Communications 4 (2005) 235–238.
[10] Y.H. Lin, C.W. Nan, Y. Liu, J. Li, T. Mizokawa, Z. Shen, High-temperature electrical transport and thermoelectric power of partially substituted $Ca_3Co_4O_9$-based ceramics, Journal of the American Ceramic Society 90 (2007) 132–136.
[11] Q. Yao, D.L. Wang, L.D. Chen, X. Shi, M. Zhou, Effects of partial substitution of transition metals for cobalt on the high-temperature thermoelectric properties of $Ca_3Co_4O_{9+\delta}$, Journal of Applied Physics 97 (2005) 103905.
[12] H.Q. Liu, X.B. Zhao, T.J. Zhu, Y. Song, F.P. Wang, Thermoelectric properties of Gd, Y co-doped $Ca_3Co_4O_{9+\delta}$, Current Applied Physics 9 (2009) 409–413.
[13] K. Park, K.Y. Ko, W.S. Seo, Thermoelectric properties of $CuAlO_2$, Journal of the European Ceramic Society 25 (2005) 2219–2222.
[14] T. Seetawan, V. Amornkitbamrung, T. Burinprakhon, S. Maensiri, P. Tongbai, K. Kurosaki, H. Muta, M. Uno, S. Yamanaka, Effect of sintering temperature on the thermoelectric properties of $Na_xCo_2O_4$, Journal of Alloys and Compounds 416 (2006) 291–295.
[15] S. Gallini, J.R. Jurado, M.T. Colomer, Combustion synthesis of nanometric powders of $LaPO_4$ and Sr-substituted $LaPO_4$, Chemistry of Materials 17 (2005) 4154–4161.
[16] K. Deshpande, A. Mukasyan, A. Varma, Direct synthesis of iron oxide nanopowders by the combustion approach: reaction mechanism and properties, Chemistry of Materials 16 (2004) 4896–4904.
[17] R.K. Lenka, T. Mahata, P.K. Sinha, A.K. Tyagi, Combustion synthesis of gadolinia-doped ceria using glycine and urea fuels, Journal of Alloys and Compounds 466 (2008) 326–329.
[18] N.P. Bansal, Z. Zhong, Combustion synthesis of $Sm_{0.5}Sr_{0.5}CoO_{3-x}$ and $La_{0.6}Sr_{0.4}CoO_{3-x}$ nanopowders for solid oxide fuel cell cathodes, Journal of Power Sources 158 (2006) 148–153.
[19] D. Wang, L. Chen, Q. Yao, J. Li, High-temperature thermoelectric properties of $Ca_3Co_4O_{9+\delta}$ with Eu substitution, Solid State Communications 129 (2004) 615.
[20] E. Woermann, A. Muan, Phase equilibria in the system CaO–cobalt oxide in air, Journal of Inorganic and Nuclear Chemistry 32 (1970) 1455–1459.
[21] A. Banerjee, S. Pal, S. Bhattacharya, B.K. Chaudhuri, H.D. Yang, Particle size and magnetic field dependent resistivity and thermoelectric power of $La_{0.5}Pb_{0.5}MnO_3$ above and below metal–insulator transition, Journal of Applied Physics 91 (2002) 5125–5134.
[22] C.M. Bhandari, Optimization of carrier concentration, in: D.M. Rowe (Ed.), in: CRC Handbook of Thermoelectrics, CRC Press, Boca Raton, 1995, pp. 43–54.
[23] G. Xu, R. Funahashi, M. Shikano, Q. Pu, B. Liu, High temperature transport properties of $Ca_{3-x}Na_xCo_4O_9$ system, Solid State Communications 124 (2002) 73–76.
[24] C.M. Bhandari, Minimizing the thermal conductivity, in: D.M. Rowe (Ed.), in: CRC Handbook of Thermoelectrics, CRC Press, Boca Raton, 1995, pp. 55–65.
[25] M. Fujisawa, T. Hata, H. Kitagawab, P. Bronsveld, Y. Suzuki, K. Hasezaki, Y. Noda, Y. Imamura, Thermoelectric properties of porous SiC/C composites, Renewable Energy 33 (2008) 309–313.
[26] L. Yang, J.S. Wu, L.T. Zhang, Synthesis of filled skutterudite compound $La_{0.75}Fe_3CoSb_{12}$ by spark plasma sintering and effect of porosity on thermoelectric properties, Journal of Alloys and Compounds 364 (2004) 83–88.
[27] K.F. Cai, J.P. Liu, C.W. Nan, X.M. Min, Effect of porosity on the thermal–electric properties of Al-doped SiC ceramics, Journal of Materials Science Letters 16 (1997) 1876–1878.